EFFECTS OF THE INJECTOR DIRECTION ON THE TEMPERATURE DISTRIBUTION DURING FILLING OF HYDROGEN TANKS

D. Melideo[(1)*], D. Baraldi[(1)], N. De Miguel Echevarria[(1)], B. Acosta Iborra[(1)]
[(1)] Joint Research Centre of the European Commission - Directorate for Energy, Transport and Westerduinweg 3, 1755 LE Petten, Netherlands

([*])Contact author: daniele.melideo@ec.europa.eu

ABSTRACT

The development of the temperature field in hydrogen tanks during the filling process has been investigated with Computational Fluid Dynamics (CFD). Measurements from experiments undertaken at the JRC GasTef facility have been used to develop and validate the CFD modelling approach. By means of the CFD calculations, the effect of injector direction on the temperature distribution has been analysed. It has been found that the dynamics of the temperature field, including the development of potentially detrimental phenomena like thermal stratification and temperature inhomogeneity e.g. hot spots, can be significantly affected by the injector orientation.

1.0 INTRODUCTION

During the filling process of hydrogen tanks of a fuel-cell powered vehicle, the gas pressure is increased significantly, typically from pressures as low as 2 MPa to more than 70 MPa. Because of the compression, the gas temperature increases and consequently the tank material temperature grows due to the heat transfer from the gas to the tank wall. The tank design temperature range is between -40°C and +85°C [1-4] and temperatures outside that range can potentially affect the mechanical behaviour of the tank materials. Moreover, the final temperature of the gas inside the vessel has a direct effect on the state of charge of the tank.

In this context, many studies especially in the last decade have been performed to investigate the temperature histories of the gas during the filling [5-27]. Many parameters affect the temperature histories e.g. the initial conditions of pressure and temperature, the pressure rise rate, the final pressure, the hydrogen pre-cooling temperature, the type and volume of the tank, and the injector configuration. Among these studies one parameter related to the injector configuration has not been thoroughly investigated, and that is the injector direction. To the authors' knowledge, only Terada and co-workers addressed that issue in the available scientific literature [29]. In their paper, they concluded that the jet direction has no effect on the gas temperature for the specific conditions that they had considered in their experimental campaign. They investigated the case where no thermal stratification occurred with a straight injector.

The objective of this paper is to enlarge Terada's investigation, by means of CFD (Computational Fluid Dynamics) simulations, and verify whether their observation could be extended to the other conditions, and more specifically to the conditions for which thermal stratification occurs already with a straight injector.

Thermal stratification inside the vessel is a phenomenon that should be avoided for several reasons. The first one is that in the case of stratification, the maximum temperature in the gas could exceed the threshold of the 85°C in the upper part of the tank e.g. hot spots, even when the average gas temperature is well below that limit. Moreover with thermal stratification, it becomes much more difficult to control and monitor the gas temperature inside the vessel compared to the case with uniform temperature distribution where one sensor is sufficient to describe the whole temperature field.

Moreover, the calculation and prediction of a stratified temperature field requires the use of 3D models (e.g. CFD) that are much more expensive and time-consuming to run compared to 0D or 1D models. The latter models can be applied only when uniform temperature fields occur to provide an almost instantaneous prediction of the temperature history. Since 0D/1D models are inherently not capable of describing the thermal stratification, avoiding the conditions for which a stratified temperature field can occur, would allow the use of the 0D/1D models in industrial environments like hydrogen re-fuelling stations.

The investigation in this paper is based on CFD simulations. A validation case has been included in the paper to assess the model accuracy in describing the relevant phenomena by comparison of experimental measurements to simulation results.

2.0 SIMULATION SET-UP

The simulations have been performed with the commercial CFD software ANSYS CFX V15.0 [30]. The CFD modelling approach has been developed and validated in a series of previous studies [31-37]. In order to capture the thermal conduction through the solid material and the changing temperature in the gas, the conjugate heat transfer model in CFX has been used.

For the advection terms the high-resolution scheme was used, while for the transient terms the 2nd order backward Euler was employed. Further details on the numerical scheme can be found in the ANSYS CFX manual [30]. A residual convergence criterion for RMS (root mean square) mass-momentum equations of 10^{-4} has been applied to ensure numerical convergence.

Since at high pressures the ideal gas law is not capable of accurately describing the pressure and the temperature field, a real gas equation of state has been used (Redlich, Kwong [38]). The gravitational source term has been included into the momentum equation and in the turbulent kinetic energy and dissipation equations to consider buoyancy effects.

The selected turbulence model is the k-ω based Shear-Stress-Transport (SST) model. It was originally designed to achieve highly accurate predictions of the onset and the amount of flow separation under adverse pressure gradients by the inclusion of transport effects into the formulation of the eddy-viscosity [39]. The full transition model is based on two transport equations, one for the flow intermittency and one for the transition onset criteria in terms of momentum thickness Reynolds number. It is called 'Gamma Theta Model' and it is the recommended transition model for general-purpose applications. It uses a new empirical correlation [40] which has been developed to cover standard bypass transition as well as flows in low free-stream turbulence environments. This built-in correlation has been extensively validated together with the SST turbulence model for a wide range of transitional flows [40].

3.0 VALIDATION CASE

Although several validation studies were already carried out in the past with the same CFD code and with the same modelling approach [31-37], a new experimental case where a strong stratification occurs has been considered to assess the model capability of accurately reproducing the relevant conditions for this investigation.

The experiment was performed in the GasTef facility of the Joint Research Centre of the European Commission [24-27, 41]. The tank is a 36 L type IV tank, with an internal polymer liner, an external carbon fiber reinforced polymer (CFRP), and stainless steel bosses. The specific experimental conditions were selected to produce a significant stratification in the tank temperature. Six positions were considered for the temperature sensors as illustrated in Figure 1: 2 sensors in the gas (Gtop in the top region of the tank and Gbot in the bottom one), 2 sensors inside the tank wall and more

specifically at the liner/CFRP interface (Mtop in the top region of the tank and Mbot in the bottom one) and 2 sensors on the external surface of the tank (Etop in the top region of the tank and Ebot in the bottom one). The top and bottom positions for the sensors were selected to provide a clear indication of the level of temperature stratification in the tank. The histories of the inlet gas conditions are described in the graphs in Figure 2.

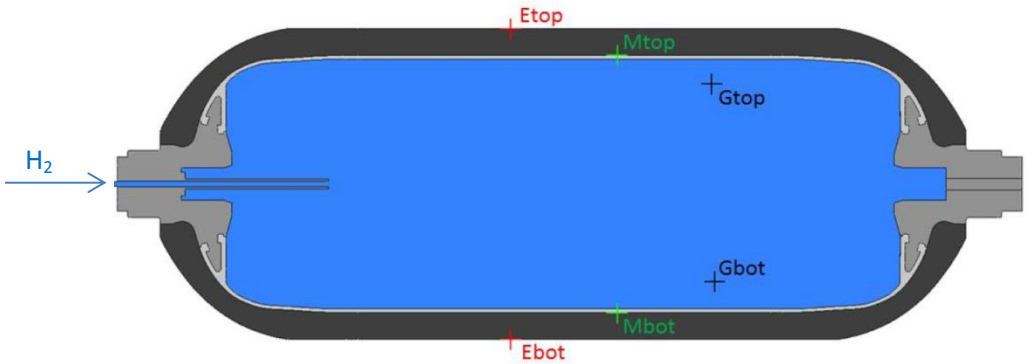

Figure 1. Position of the sensors in the gas (black), at the liner/CFRP interface (green), and on the outer surface of the tank (red).

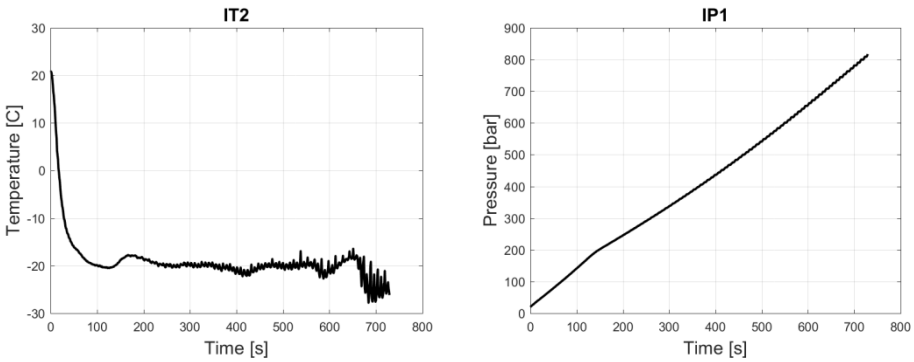

Figure 2. Temperature and pressure history of the inlet gas.

The test parameters are reported in Table 1.

Table 1. Test parameters.

Case	Injector direction	Initial T [°C]	Final P [bar]	Total time [s]
Validation case	Straight	21.75	817.25	730

As described in Figure 3, the agreement between the experiment and the simulation is good until 400 s for the gas temperature, including the abrupt beginning of the thermal stratification in the gas at about 160 s. In the last 250 s, a progressive discrepancy can be observed between the simulation data and the experimental measurements and the final difference is within 5 degrees in the gas, and within 2 degrees in the tank material. Although the agreement in the second part of the simulation is not as good as in the first part, the overall accuracy of the CFD model can be considered sufficient for this investigation that aims at identifying some clear tendencies in the behaviour of the temperature field.

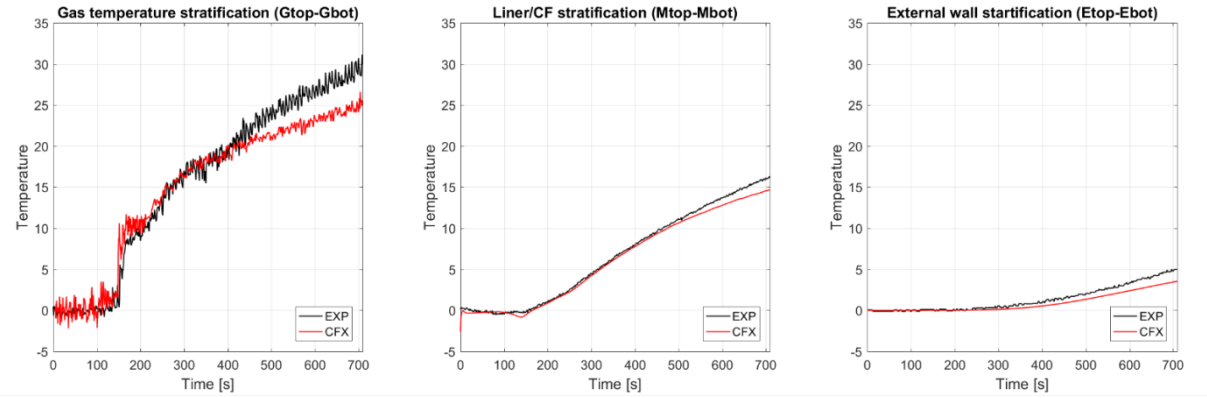

Figure 3. Comparison between experiment and simulation for the temperature difference between top and bottom position in the gas, at the liner/CFRP interface, and on the external wall of the tank.

4.0 SELECTED CASES

The list of the injector orientation cases that are investigated numerically is shown in Table 2 including the values for the relevant parameters. The first letter of the case name indicates the type of injector: S for the straight injector, D for the downward injector (with an angle of 45˚) and U for the upward injector (with an angle of 45˚). The second part of the case name indicates the initial/ambient temperature. The pre-cooling inlet gas temperature is -20° and the initial pressure is 2 MPa for all cases. Three initial temperatures have been selected for the gas and the tank: 0°C, 30°C, and 35°C. The initial temperatures at 30°C and 35°C were selected to investigate cases with longer filling times where thermal stratification is more likely to occur; the purpose of the initial temperature at 0°C case is to analyse the effect of the injection direction with lower initial/ambient temperature. The values of the final pressure and the average pressure rise rate (APRR) have been selected from the SAE tables [2].

Table 2. List of the simulated cases with relevant parameters (APRR=Average Pressure Rise Rate).

Case	Injector direction	Initial T [˚C]	Final P [MPa]	APPR [MPa/min]	Total time [min]
S_T30	Straight	30	73.6	5.0	14.32
S_T35	Straight	35	74.5	3.9	18.59
S_T00	Straight	0	66.4	15.3	4.21
U_T30	Upward	30	73.6	5.0	14.32
U_T35	Upward	35	74.5	3.9	18.59
U_T00	Upward	0	66.4	15.3	4.21
D_T30	Downward	30	73.6	5.0	14.32
D_T35	Downward	35	74.5	3.9	18.59
D_T00	Downward	0	66.4	15.3	4.21

5.0 SIMULATION RESULTS AND DISCUSSION

Given the same initial conditions, the average gas temperature is very similar even if the injector direction is different as described in Figure 4 for the cases with the 30°C initial temperature: the average gas temperature differs by only few degrees in the 3 cases. Despite the similar average gas

temperature, the temperature distribution and stratification change significantly with the injector configuration as described in Figure 5.

The temperature difference between the top positions and the bottom positions (in the gas, at the liner/CFRP interface and on the outer surface of the tank) for the cases with initial temperature of 30°C, 35°C, and 0°C is illustrated in Figure 5, Figure 9, and Figure 10 respectively.

As shown in the left-hand side of Figure 5 for the cases with initial temperature of 30°C, the gas temperature is almost uniform for about 150 s, for about 180 s, and for about 300 s with the downward injector, with the straight injector and with the upward injector respectively. The first effect of a downward injector is to anticipate the beginning of the thermal stratification compared to the straight configuration while the opposite occurs with the upward injector. In the latter configuration, the cold jet results in lower temperature in the upper section of the tank up to almost 500 s. The thermal stratification is strongly enhanced by the downward injector while it is significantly reduced by the upward shape as demonstrated by the final gas temperature difference of about 62°C, 26°C, and 7°C in the downward, straight and upward configuration respectively. From the qualitatively point of view, a similar effect of the injector direction on the final temperatures can be found at the liner/CFRP interface and on the outer surface at the end of the filling process.

An interesting behaviour can be identified by comparing the temperature difference histories in the gas and at the liner/CFRP interface in Figure 5. Contrary to the other configurations, for the upward configuration the temperature difference is negative in the gas in the first 500 seconds, while it is positive for most of that time at the interface liner/CFRP. That means that in the first 500 s the temperature is smaller in the upper region than in the lower region for the gas while the opposite occurs for the tank material. The behaviour in the gas temperature can be explained with the effect of the changing direction of the cooling jet as illustrated in Figure *8*. The reason for the counter-intuitive behaviour in the material can be found in the heat transfer process from the warm gas to the colder material. The heat transfer depends on the temperature difference between the gas and the liner and on the heat transfer coefficient. The upward jet impinging on the top surface of the liner creates a region in the top part of the tank where the flow velocity and turbulence is larger than in the lower part. That causes a larger heat transfer coefficient between the gas and the liner in the upper region than in the lower region for the first 500 s as shown in the heat transfer coefficient history for the upward configuration in Figure 6.

In Figure *7*, the flow velocity at the exit of the injector is described for the straight configurations. The inlet flow velocity (at the exit along the centreline of the injector) is driven by the ratio between the compressor pressure and the tank pressure and it does not depend on the direction of the injector. Since the pressure ratio decreases with time during the filling, the flow velocity at the inlet decreases as illustrated in Figure *7*. The effect of buoyancy tends to bend downward the direction of the incoming cold jet and that effect becomes more relevant with the decreasing jet velocity. That effect is clearly shown at 500 s in Figure 8. Both the decreased velocity and the bent direction of the jet affect the wall heat transfer coefficient and at about 500 s the heat transfer coefficients in the bottom wall of the tank and in the top wall have similar values for the upward configuration (Figure 6).

Subsequently the jet is bent even further down towards the lower wall of the tank as depicted at 859 s in Figure 8 and the heat transfer coefficient is larger at the bottom wall than at the top one. Consistently with that, the temperature difference at the liner/CFRP interface changes sign in the second half of the process as shown in Figure 5.

The temperature field history in the gas and in the tank material can be explained with the interactions of the jet velocity and direction, the buoyancy effects, and the heat transfer coefficient/process also for the other cases. The direction of the jet is driven by the injector geometry and by 2 competing factors: the jet speed and the buoyancy effect. The jet increases the heat transfer coefficient on the wall on which it is impinging and the increased heat transfer generates higher temperature in the tank material.

A similar behaviour is confirmed also for the cases with 35°C initial temperature as depicted in Figure 9. For the cases with 0°C initial temperature, the filling time is much shorter, the APRR (and the jet velocity) is much larger than for the other 2 cases, and the temperature differences are smaller as illustrated in Figure 10. Remarkably for that case the gas stratification is almost completely eliminated with the upward injector.

The different temperature fields that are generated by the upward, straight, and downward injector at the end of the filling process with initial temperature of 30°C can be appreciated in Figure 11.

Fluctuations are typical features of the jet flow pattern that is characterized by flow instabilities [28]. The flow fluctuations produce fluctuations in the temperature field (due to the oscillations of the borders between regions at different temperatures) as shown in all figures with the gas temperature differences. Obviously, those fluctuations are completely absent for the temperature of the liner/CFRP interface and on the outer surface of the tank. Flow and temperature difference fluctuations have a direct impact on the heat transfer coefficient, causing larger fluctuations in the heat transfer coefficient histories as illustrated in Figure *6*.

The findings on the effect of the jet direction in this work are apparently different from the observations of Terada and co-workers [29]. In their experimental campaign, they changed the jet direction and they did not record any significant difference in the gas temperature rise for the difference jet configurations. Several differences in the relevant conditions between the Terada's set-up and that in this paper can be identified: the injector diameter (5.2 mm in Terada's and 6 mm in this work), the tank volume (65 L in Terada's, 36 L in this work), the final pressure (35MPa in Terada's and ~70 MPa in this work). In Terada's experiment, no local in-homogeneities occurred with the straight configuration and for that case, the effect of the jet direction was negligible. In this work, the conditions have been selected on purpose to analyse cases with stratification occurring with a straight injector. That is the main difference with Terada's investigation and that leads to different conclusions.

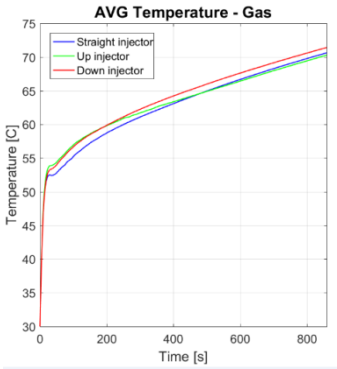

Figure 4. History of average gas temperature for the cases with 30°C initial temperature.

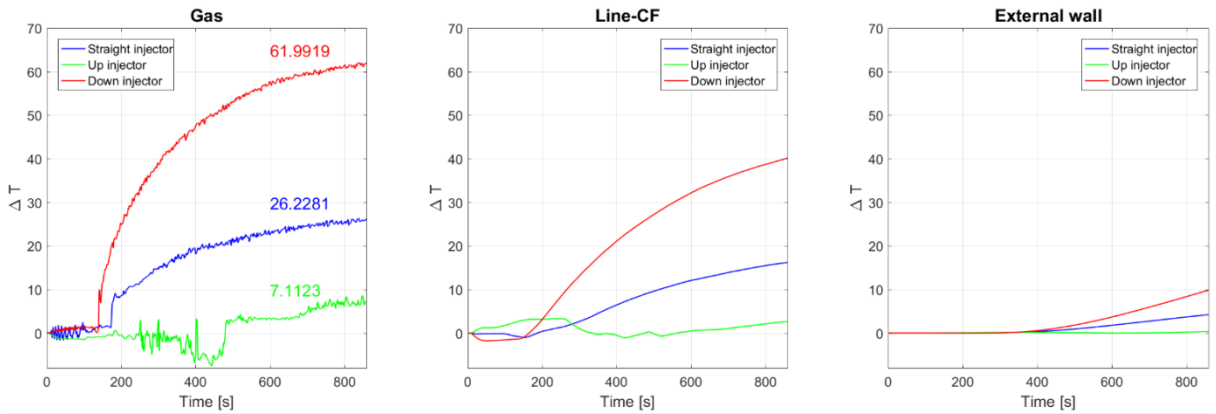

Figure 5. Histories of temperature difference between top and bottom position in the gas (left-hand side), at the liner-CFRP interface (centre), and on the outer surface (right-hand side) of the tank for the cases with 30°C initial temperature.

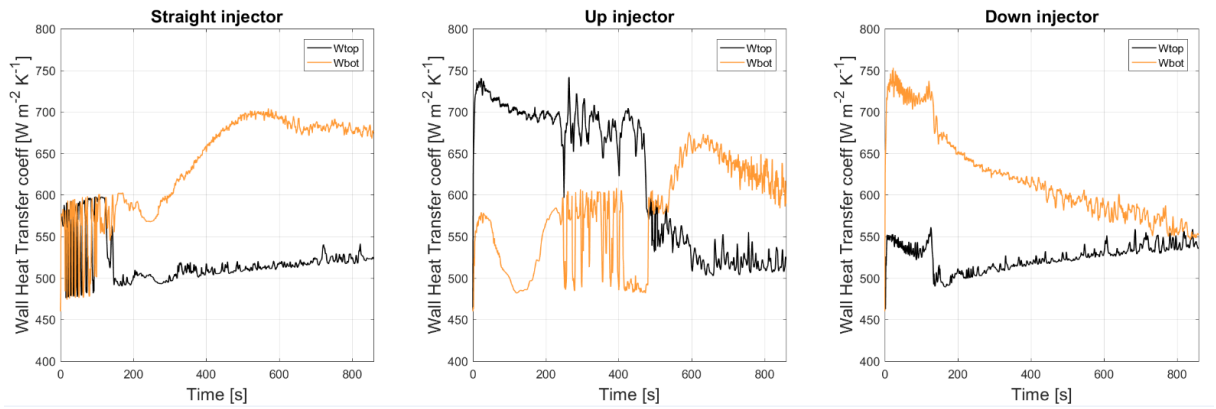

Figure 6. History of the heat transfer coefficient at the inner surface of the liner in contact with the gas for the cases with 30°C initial temperature.

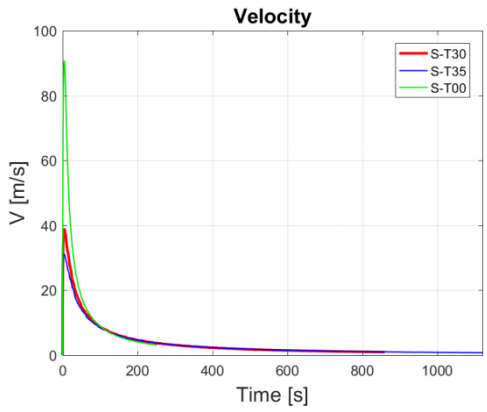

Figure 7. Histories of flow velocity close at the exit of the injector for the straight configurations.

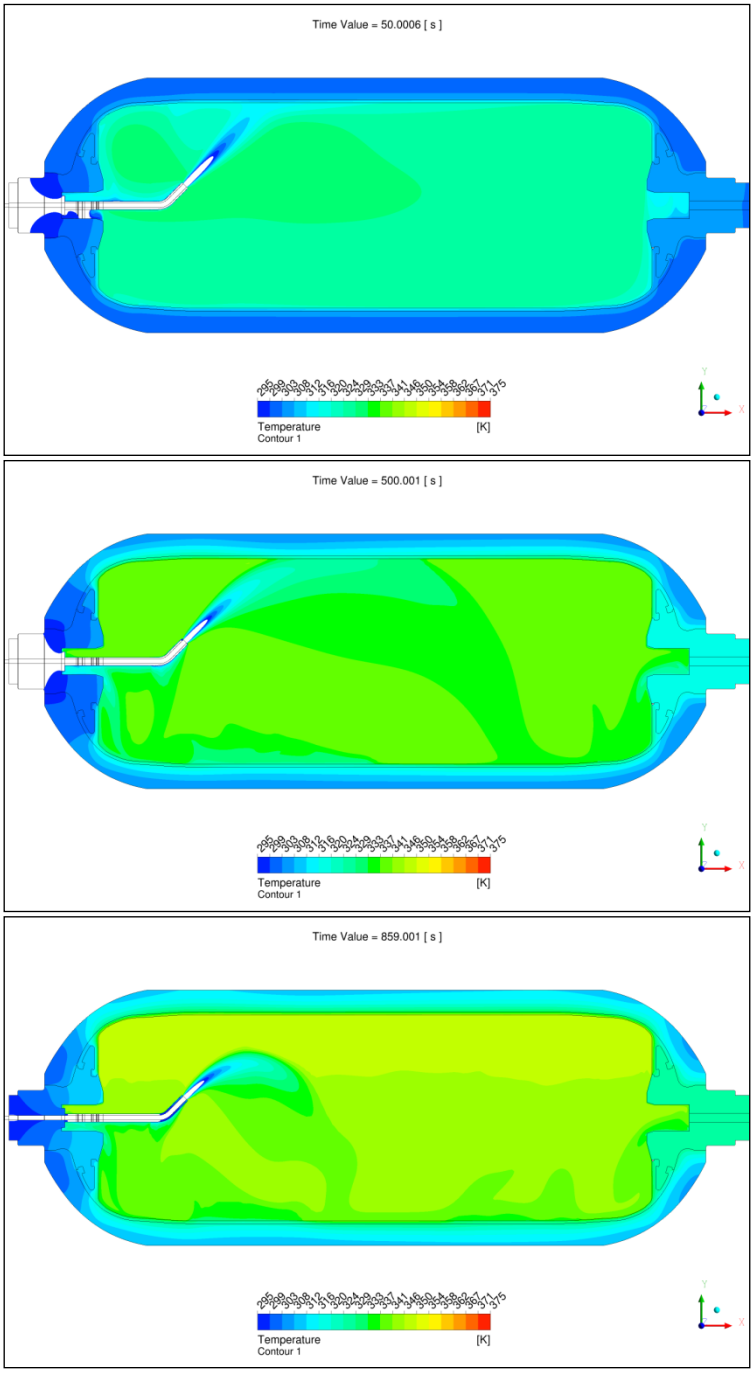

Figure 8. Temperature field for the case with 30°C initial temperature and with upward injector at 50 s, 500s, and 859 s.

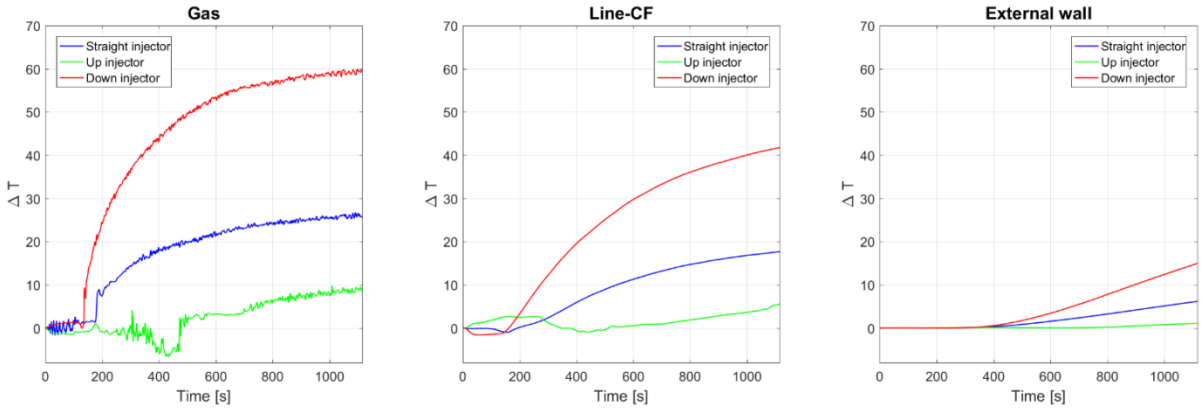

Figure 9. Histories of temperature difference between top and bottom position in the gas (left-hand side), at the liner-CFRP interface (centre), and on the outer surface (right-hand side) of the tank for the cases with 35°C initial temperature.

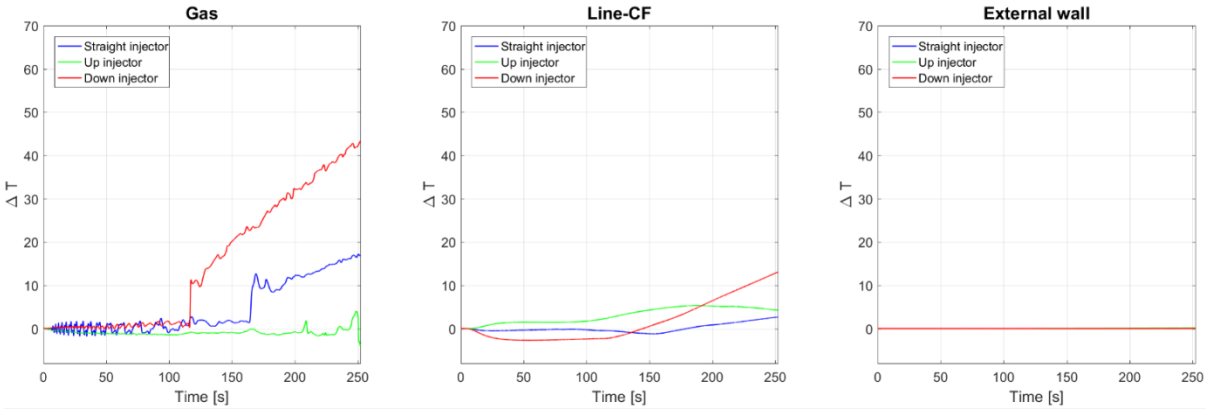

Figure 10. Histories of temperature difference between top and bottom position in the gas (left-hand side), at the liner-CFRP interface (centre), and on the outer surface (right-hand side) of the tank for the cases with 0°C initial temperature.

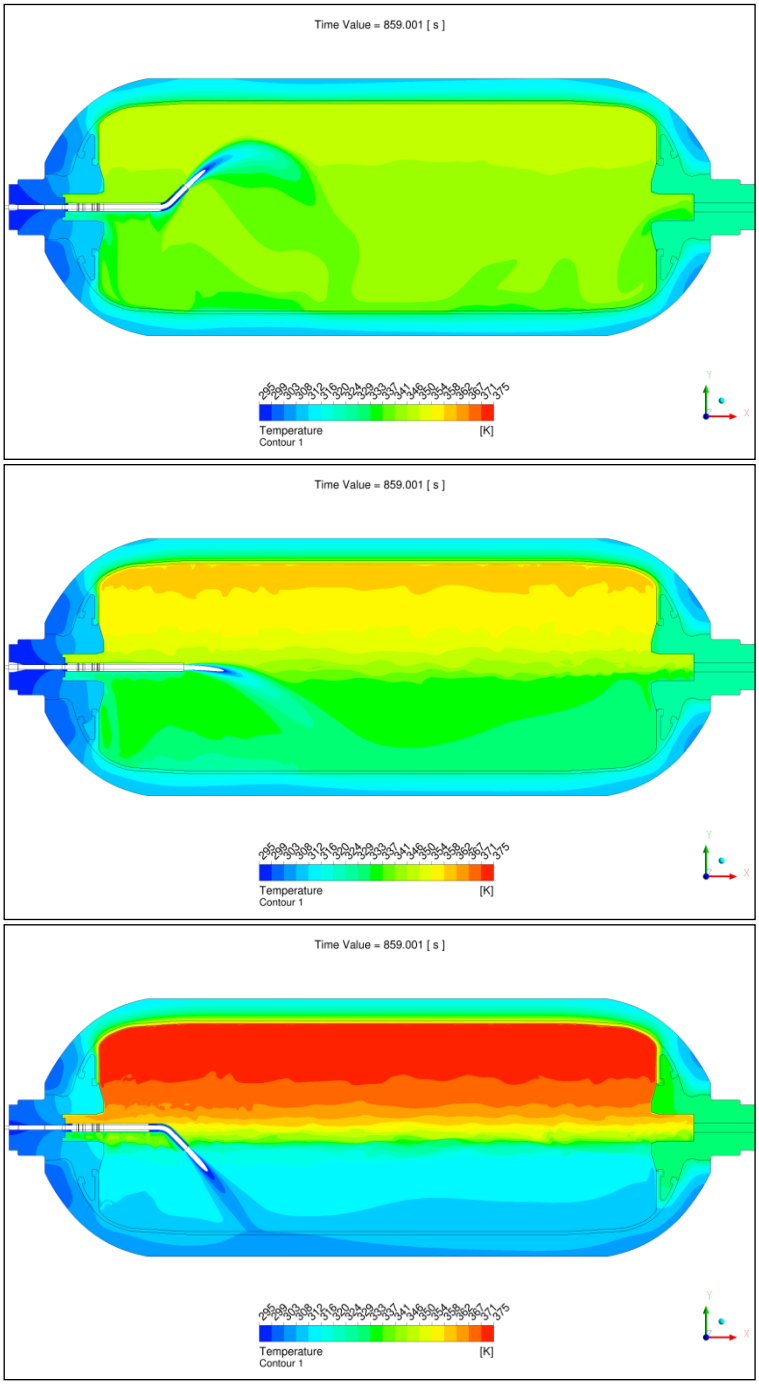

Figure 11. Temperature field for the cases with 30°C initial temperature with upward, straight and downward injector at the end of the filling process (859 s).

6.0 CONCLUSIONS

CFD simulations of the filling process of a hydrogen tank were performed for different initial conditions and for different directions of the gas injector. The conditions of the simulated cases were selected from the SAE tables with the purpose to generate and investigate a stratified temperature field as temperature in-homogeneities are not desirable during the filling. Three different injector configurations were considered in the analysis: a straight injector, an upward injector and a downward injector.

When stratification occurs with the straight injector, the temperature in-homogeneities increase significantly with the downward injector and their onset is anticipated. On the contrary with the upward configuration the onset of the stratification is strongly delayed or completely averted, and the temperature difference between the top and the bottom part of the tank are strongly reduced or eliminated, depending on the case.

The above finding is not consistent with Terada's work [29] where no effect of the jet direction on the temperature distribution was observed. Significant differences for the conditions of the filling between Terada's work and this investigation justify the discrepancy between the conclusions in the 2 investigations. On the contrary to Terada's study, the conditions in this investigation were selected to create a significant thermal stratification.

7.0 ACKNOWLEDGEMENTS

This work has been performed at the Joint Research Centre of the European Commission in Petten (NL). The authors would like to acknowledge and thank all colleagues working on GasTeF facility Frederik Harskamp, Kevin Goblet, Christian Bonato. The authors would like also to thank the partners of the Fuel Cell Hydrogen Joint Undertaking co-funded HyTransfer project (FCH JU grant agreement 2012-1-325277) for the interesting and fruitful discussions on the topic.

8.0 REFERENCES

1. GTR ECE/TRANS/WP.29/2013/41. Proposal for a global technical regulation (GTR) on hydrogen and fuel cell vehicles. June 2013.
2. SAE J2579. Standard for fuel systems in fuel cell and other hydrogen vehicles. March 2013.
3. Commission Regulation (EU) No 406/2010 of 26 April 2010. Implementing regulation (EC) No 79/2009 of the European parliament and of the council on type-approval of hydrogen powered motor vehicles. May 2010.
4. SAE J2601. Fuelling protocols for light duty gaseous hydrogen surface vehicles. SAE international; July 2014, Dec 2016.
5. Maus S. Modellierung und simulation der betankung von fahrzeugbeh€altern mit komprimiertem wasserstoff. Du¨ sseldorf: Verlag; 2007 (879), Fortschr.-Ber., VDI Reihe 3VDI.
6. Monde M, Kosaka M. Understanding of thermal characteristics of fueling hydrogen high pressure tanks and governing parameters. SAE Int J Alt Power 2013;2(1):61-67.
7. Dicken CJB, Merida W. Modeling the transient temperature distribution within a hydrogen cylinder during refueling. Numer Heat Transf Part A Appl 2007;53:685-708.
8. Kim SC, Lee SH, Yoon KB. Thermal characteristics during hydrogen fueling process of type IV cylinder. Int J Hydrogen Energy 2010;35:6830-5.
9. Suryan A, Kim HD, Setoguchi T. Three dimensional numerical computations on the fast filling of a hydrogen tank under different conditions. Int J Hydrogen Energy 2012;37:7600-11.

10. Liu Y, Zheng J, Xu P, Zhao Y, Li L, Liu P, et al. Numerical simulation on fast filling of hydrogen for composite storage cylinders. In: Proc. PVP2008 ASME press. Vessel. Pip. Div. Conf.; 2008.
11. Demael E, Liquide A, Weber M, Renault P. Experimental and numerical evaluation of transient temperature distribution inside a cylinder during fast filling for H2 applications. In: Proceedings of the WHEC, May 16.-21. 2010, Essen, vol. 78; 2010. p. 1e7.
12. Immel R, Mack-Gardner A. Development and validation of a numerical thermal simulation model for compressed hydrogen gas storage tanks. SAE Int J Engines 2011; 4:1850e61.
13. Y. Takagi, N. Sugie, K. Takeda, Y. Okano, T. Eguchi, K. Hirota, Numerical investigation of the thermal behaviour in a hydrogen tank during fast filling process. Asme/Jsme 2011, Honolulu, Hawaii, USA.
14. Ranong CN, Maus S, Hapke J, Fieg G, Wenger D. Approach for the determination of heat transfer coefficients for filling processes of pressure vessels with compressed gaseous media. Heat Transf Eng 2011;32(2):127e32.
15. Li Q, Zhou J, Chang Q, Xing W. Effects of geometry and inconstant mass flow rate on temperatures within a pressurized hydrogen cylinder during refueling. Int J Hydrogen Energy 2012;37(7):6043e52.
16. Zhao L, Liu Y, Yang J, Zhao Y, Zheng J, Bie H, et al. Numerical simulation of temperature rise within hydrogen vehicle cylinder during refueling. Int J Hydrogen Energy 2010; 35:8092-100.
17. Zhao Y, Liu G, Liu Y, Zheng J, Chen Y, Zhao L, et al. Numerical study on fast filling of 70 MPa type III cylinder for hydrogen vehicle. Int J Hydrogen Energy 2012; 37:17517-22.
18. Suryan A, Kim HD, Setoguchi T. Comparative study of turbulence models performance for refueling of compressed hydrogen tanks. Int J Hydrogen Energy 2013; 38:9562-9.
19. Zheng J, Guo J, Yang J, Zhao Y, Zhao L, Pan X, et al. Experimental and numerical study on temperature rise within a 70 MPa type III cylinder during fast refueling. Int J Hydrogen Energy 2013;38:10956-62.
20. Setoguchi T, Alam MMA, Monde M, Kim HD. Characteristics of turbulent confined jets during fast filling of H2 tank at high pressure. Aeroacoustic 2013; 12:455-74.
21. Wang G, Zhou J, Hu S, Dong S, Wei P. Investigations of filling mass with the dependence of heat transfer during fast filling of hydrogen cylinders. Int J Hydrogen Energy 2014;39(9):4380-8.
22. Wang L, Zheng C, Wei S, Wang B, Wei Z. Thermo-mechanical investigation of composite high-pressure hydrogen storage cylinder during fast filling. Int J Hydrogen Energy 2015;40:6853-9.
23. Johnson T, Bozinoski R, Ye J, Sartor G, Zheng J, Yang J. Thermal model development and validation for rapid filling of high pressure hydrogen tanks. Int J Hydrogen Energy 2015;40:9803-14.
24. De Miguel N, Ortiz Cebolla R, Acosta B, Moretto P, Harskamp F, Bonato C. Compressed hydrogen tanks for onboard application: thermal behaviour during cycling. Int J Hydrogen Energy 2015;40(19):6449-58.
25. De Miguel N, Acosta B, Moretto P, Ortiz Cebolla R. The effect of defueling rate on the temperature evolution of on-board hydrogen tanks. Int J Hydrogen Energy 2015;40(42):14768-74.
26. Ortiz Cebolla R, Acosta B, Moretto P, de Miguel Echevarria N. Effect of precooled inlet gas and mass flow rate on final state of charge during hydrogen refuelling. Int J Hydrogen Energy 2015;40(13):4698-706.
27. De Miguel N, Acosta B, Moretto P, Ortiz Cebolla R. Influence of the gas injector configuration on the temperature evolution during refueling of on-board hydrogen tanks. Int J Hydrogen Energy2016;41(11): 19447–19454
28. Ball CG, Fellouah H, Pollard A. The flow field in turbulent round free jets. Progress in Aerospace Sciences. 50 (2012) 1–26.
29. Terada T, Yoshimura H, Tamura Y, Mitsuishi H, Watanabe S. Thermal behavior in hydrogen storage tank for FCV on fast filling (2nd report). SAE Technical Paper 2008-01-0463. 2008.
30. ANSYS CFX. User's guide. Release 15.0. ANSYS Inc. 2014.

31. Heitsch M, Baraldi D, Moretto P. Numerical investigations on the fast filling of hydrogen tanks. Int J Hydrogen Energy February 2011; 36(3):2606-12.
32. Galassi MC, Baraldi D, Acosta Iborra B, Moretto P. CFD analysis of fast filling scenarios for 70 MPa hydrogen type IV tanks. Int J Hydrogen Energy 2012;37(8):6886-92.
33. Melideo D, Baraldi D, Galassi MC, Ortiz Cebolla R, Acosta Iborra B, Moretto P. CFD model performance benchmark of fast filling simulations of hydrogen tanks with pre-cooling. Int J Hydrogen Energy 2014;39(9):4389-95.
34. Galassi MC, Papanikolaou E, Heitsch M, Baraldi D, Iborra BA, Moretto P. Assessment of CFD models for hydrogen fast filling simulations. Int J Hydrogen Energy2013; 39(11):6252-60.
35. Melideo D, Baraldi D. Erratum to "CFD analysis of fast filling strategies for hydrogen tanks and their effects on keyparameters" [Int. J. Hydrogen Energy 40 (2015) 735-745]. Int J Hydrogen Energy 2015; 40:6260-8.
36. Melideo D, Baraldi D, Acosta-Iborra B, Ortiz Cebolla R, Moretto P. CFD simulations of filling and emptying of hydrogen tanks. Int. J. Hydrogen Energy. In press. http://dx.doi.org/10.1016/j.ijhydene.2016.05.262
37. Bourgeois T,Brachmann T, Barth F, Ammouri F, Baraldi D, Melideo D, Acosta-Iborra B, Zaepffel D, Saury D, Lemonnier D. Optimization of hydrogen vehicle refuelling requirements. In press. http://dx.doi.org/10.1016/j.ijhydene.2017.01.165
38. Redlich O, Kwong JNS. On the thermodynamics of solutions:V. An equation of state: fugacity of gaseous solutions. Chem Rev 1949; 44:233-44.
39. Menter FR. 1994 Two-equation eddy-viscosity turbulence models for engineering applications. AIAA J 32:1598–605.
40. Langtry RB, Menter FR. 2009 Correlation-based transition modeling for unstructured parallelized computational fluid dynamics codes. AIAA J 2009; 47:2894–906.
41. Ortiz Cebolla R, Acosta B, Moretto P, Frischauf N, Harskamp F, Bonato C, et al. Hydrogen tank first filling experiments at the JRC-IET GasTeF facility. Int J Hydrogen Energy 2014;39:6261-66267.